International Communications in Heat and Mass Transfer 116 (2020) 104653

Contents lists available at ScienceDirect

International Communications in Heat and Mass Transfer

journal homepage: www.elsevier.com/locate/ichmt

Molecular dynamics simulation of ferro-nanofluid flow in a microchannel in the presence of external electric field: Effects of Fe_3O_4 nanoparticles

Reza Balali Dehkordi[a], Davood Toghraie[a,*], Mohammad Hashemian[a], Farshid Aghadavoudi[a], Mohammad Akbari[b]

[a] Department of Mechanical Engineering, Khomeinishahr Branch, Islamic Azad University, Khomeinishahr, Iran
[b] Department of Mechanical Engineering, Najafabad Branch, Islamic Azad University, Najafabad, Iran

ARTICLE INFO

Keywords:
Molecular dynamics
Nanofluid
Water/Fe_3O_4
Water
Microchannel

ABSTRACT

In this study, the effect of nanoparticle variation on water/Fe3O4 nanofluid manner in the presence of an external electric field reported. The results of the physical properties of these structures were estimated by LAMMPS software. The results of these simulations are used in the design of electronic equipment in which nanofluids are used as refrigerants in their structures. Physically, for studying the nanofluid atomic manner, we calculated parameters such as potential energy, density, velocity, and temperature profiles of atomic structures. Our results showed that the nanoparticle is an important parameter to nanofluid movement in a microchannel. Numerically, by increasing the nanoparticle number from 1 to 3, the maximum rate of density, velocity, and temperature profiles increases to 1.675 g/cm^3, 0.012 Å/ps, and 712 K rates, respectively. Moreover, by increasing the nanoparticle radius, the number density, velocity, and temperature of water/Fe_3O_4 nanofluids increase. So we conclude that, by adding nanoparticles to base fluid in the presence of the external electric field, the heat transfer will occur with higher quality.

1. Introduction

Different fluids are commonly used as heat conductors in thermal applications. Such applications, in which fluids have a significant role, are heat conduction systems, cooling systems in electronic, air conditioning systems, and many other important systems [1–4]. In all of the common applications, the fluid thermal conductivity coefficient has an important effect on the operation of the target system. For this reason, engineers have worked on designing advanced heat transfer fluids which have higher thermal conductivities than common fluids. Many types of research were made on heat conduction enhancement of fluids through the physical optimization of these structures. Historically, in 1995, Choi designed a surprising class of fluids that was depended on suspending metallic nanoparticles. These nanoparticle sizes are less than 100 nm, which inserted into heat transfer fluids [5,6]. So, the nanofluid term was used to define a mixture fluid that contains nanoparticles. The idea of inserting solid substances in common fluids was first designed by Maxwell's researches more than 100 years ago [7]. It was later used to disperse mm, and μm sized particles in fluids by Ahuja in 1975, Liu et al. in 1988, and Argonne National Laboratory researchers in 1992 [8–12]. These researches were depended on the high thermal conductivity of metal substances at 300 K compared to common fluids [13,14]. Therefore, by inserting metallic nanoparticles in a common fluid, its thermal manner is expected to be improved. Furthermore, the atomic manner of the nanofluid structure is a very important factor in thermal behavior.

Today, understanding the atomic manner of fluid/nanofluid has an important role in many applications [15]. Numerous academic researches have been conducted to understand fluid' nanofluid atomic manner. Experimentally, various nanochannels/microchannels which were made of different atoms have been examined [16–22]. More than conventional experimental methods, the MD method is used to study nanofluids [23]. MD method is the most important type of computer simulation that is capable to predict the atomic behavior of a variety of structures [24–26]. This computational method is widely used for studying the thermal and atomic manner of structures [27–32]. This computational method is capable of simulating and predicting atomic structure phase transition and simulation thermal process such as atomic boiling of liquids [33–38]. Furthermore, in numerous papers, researchers tried to study the nano/microscale fluid displacement with the MD approach. Fluids, which are simulated in nano/micro environment, possess different atomic manners in comparison with the

* Corresponding author at: Department of Mechanical Engineering, Islamic Azad University, Khomeinishahr Branch, Khomeinishahr 84175-119, Iran.
E-mail address: Toghraee@iaukhsh.ac.ir (D. Toghraie).

https://doi.org/10.1016/j.icheatmasstransfer.2020.104653

Nomenclature

F_{ij}	Intermolecular force on molecule i by molecule j
F_R	Replusive force
F_A	Attraction force
m	Atom mass
r_c	Cutoff distance
r_i	Position of atom i
t	Time step
T	Temperature
v_i	Velocity of atom i
a_i	acceleration of atom i
U	Interaction potential
k_B	Boltzman constant
N	Number of atoms
K_r	Oscillator constant
k_θ	Oscillator constant
r_0	Equilibrium rate of atomic bond
θ_0	Equilibrium rate of atomic angle

Greek symbols

ε	Energy parameter in Lennard-Jones (LJ) potential
σ	Length parameter of LJ potential
Δ	Delta deviation

fluids in macroscale samples. In nano/micro scales, the equilibration of the interatomic forces involved in the nano/micro system does not occur. The fluid velocity is appropriate to the wall velocity at the interface of these structures, which is called no-slip boundary condition and validated by several scientific reports in macroscale systems. However, this condition is not valid in nanoscale structures. That is, the velocity of nanofluid is not equal to the wall velocity in these structures, and this manner is called the slip manner. Physically, Witharana et al. and Chen et al. [39,40] showed that, knowledge of the atomic behavior of nanofluids is an important parameter in deciding their performance for thermodynamic applications. The previous studies showed appreciable increases in nanofluid thermal properties over those of the base-fluid, particularly the heat flux and heat transfer coefficient, have been largely improved by this procedure. Furthermore, in fluid studies, adding nanoparticles to base-fluid cause phase transition of the base-fluid in a shorter time and with more reality. Therefore, by inserting nanostructures in a common fluid, its thermal manner is expected to be improved. For studying the fluid and nanofluid manner on large scale, the continuum approach usually is used based on the continuum structure rules [41–45]. However, this approach is not valid in nanostructures, where the atomic free path is appropriate to the characteristic size of the simulation box. Therefore, the atomic methods were defined. The Molecular Dynamics (MD) method is a computational approach that defines a view of the displacement of the atoms by estimating the interatomic force of atoms over simulation time. With the extension of nanofluid applications, the MD method has become an exact approach for studying fluid flow in nano/microscale structures. So, in this computational study, the effect of nanoparticle number variation on water/Fe_3O_4 nanofluid manner is reported in the presence of an external electric field. There is the electric field in lots of electrical equipment, so this external factor is implemented in our simulation box and we study the effect of this field on nanofluid atomic behavior. Furthermore, the nanoparticle number variation is another important parameter in nanofluid atomic behavior, which has not been studied in previous researches. The results of the physical properties of these structures were estimated by LAMMPS software. Theoretically, to study the nanofluid atomic manner, parameters such as potential energy, density, velocity, and temperature profiles of atomic structures were calculated.

2. Computational method

In our research, we used the MD approach to study water/Fe3O4 nanofluid atomic manner inside a Cu microchannel. MD computational method is an approach for predicting the dynamical movement of particles. In this approach, the particles interacted and moved to other coordination with new velocity. In this method, the position r_i(t) and the momentum p_i(t)are obtained by solving Newton's equation [24],

$$F_i = m_i a_i = m_i \frac{d^2 r_i}{dt^2} \tag{1}$$

The momentum p_i can be defined as the following equation [24],

$$P_i = m_i v_i \tag{2}$$

Also, the interatomic forces are related to the potential function as (3) equation [24],

$$\frac{dU}{dr_i} = -\dot{P}_i = -m_i a_i = -F_i \tag{3}$$

Finally, in MD simulations, the motion equations can be calculated by the Verlet algorithm [46,47],

$$r(t + \Delta t) = r(t) + v(t)\Delta t + \frac{1}{2}a(t)\Delta t^2 + O(\Delta t^4) \tag{4}$$

$$v(t + \Delta t) = v(t) + \frac{a(t) + a(t + \Delta t)}{2}\Delta t + O(\Delta t^2) \tag{5}$$

The temperature of atoms in our MD simulation is another important physical parameter. For estimating this parameter, the average kinetic energy is calculated in this equation [24],

$$\frac{1}{2}mv^2 = \frac{3}{2}k_b T \tag{6}$$

Base on Eq. (6), the instantaneous temperature fluctuant is obtained by the following equation [24],

$$T(t) = \sum_i^N \frac{m_i v_i^2(t)}{k_B N} \tag{7}$$

where N is the number of degrees of freedom of the atomic system. In this computational study, all simulations were done with a Large-scale Atomic/Molecular Massively Parallel Simulator (LAMMPS) package released by Sandia National Laboratories (SNL) [48–50]. Historically, this MD simulation package designed in the 1990s. To use this simulation package for studying water/Fe_3O_4 nanofluid physical manner, the first Cu ideal microchannel with 0.75*0.3*0.3 μm^3 was simulated at initial temperature (T = 300 K). Cu atoms in definition regions are rigid. In the next step, water/Fe_3O_4 nanofluid with one Fe_3O_4 nanoparticle simulated. In nanofluid atomic structure, water molecules displacement rather each other is a function of simulation time, but Fe_3O_4 nanoparticles are rigid and don't move rather than each other. In the nanofluid structure, Fe_3O_4 nanoparticle fixed in the middle of the microchannel. This initial atomic arrangement depicted in Fig. 1. This figure shows the simulation box, which was visualized by Open Visualization Tool (OVITO) software [51].

In our MD simulations, periodic conditions were implemented in x and y directions and fixed one used for z-direction. Furthermore, for setting the initial temperature (T = 300 K), the Nose-Hoover thermostat was used on all atoms with a 0.01 K temperature damping rate in the simulation box [52–54]. The Nose–Hoover thermostat is a deterministic algorithm for constant temperature molecular dynamics simulations. It was originally developed by Nos and was improved further by Hoover. In the second step, external force equals 0.002 eV/Å

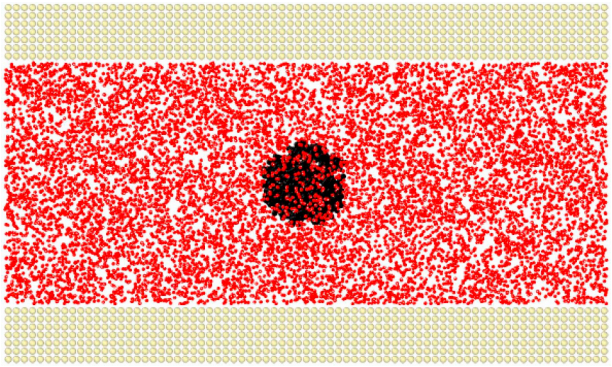

Fig. 1. Schematic of Cu microchannel and water/ Fe_3O_4 nanofluid simulated with LAMMPS package.

magnitude inserted to water/ Fe_3O_4 nanofluid, and the NVE ensemble was used to estimate the atomic manner of water/Fe_3O_4 nanofluid in Cu microchannel. The electric field is another external force source in our MD simulation. This external parameter inserted to water/Fe_3O_4 nanofluid atoms in flow direction and by below equation:

$$F = qE\ cos(\omega t) \tag{8}$$

In Eq. (1), q is the electric charge, E is the electric field magnitude, and ω is the external filed frequency. Furthermore, empirical models were used for computational studies of water molecules. SPC, SPC/E, TIP3P, and TIP4P are useful models for MD simulation of water atomic structure. In these common models, 3–5 interaction sites were used. In SPC/E one, three sites were used for the electrostatic interactions, and the positive charges on the H atoms were equilibrated by a negative charge which defined to the O atom [55,56]. Furthermore, the non-bonding interactions between two water molecules were simulated by Lennard-Jones (LJ) equation with just a single interaction point per molecule centered on the oxygen atom. The LJ equation is a basic equation that describes the interaction between particles. A form of this equation was first defined by John Lennard-Jones in 1924 [57]. The common equation of LJ formalism is [57],

$$U(r) = 4\varepsilon\left[\left(\frac{\sigma}{r_{ij}}\right)^{12} - \left(\frac{\sigma}{r_{ij}}\right)^{6}\right] \qquad r \ll r \tag{9}$$

In Eq. (9), ε is the depth of the potential well, σ is the distance at which the potential is zero, and r_{ij} is the distance between the atoms. In MD simulations, both ε and σ parameters depend on the type of the particles, which arranged in the simulation box. Furthermore, the bond and angle strength stretch in the SPC/E model is defined by harmonic oscillator equations as [55]:

$$E_r = \frac{1}{2}k_r(r - r_0) \tag{10}$$

$$E_\theta = \frac{1}{2}k_\theta(\theta - \theta_0) \tag{11}$$

In Eqs. (10) and (11), K_r and K_θ are oscillator constants. r_0 and θ_0 are the equilibrium rate of atomic bond and angle, respectively. In SPC/E model, the r_0 of OH bond is equal 1.0 $\AA$ and θ_0 of HOH angle is equal 109.47°. In this common model, all atomic interactions which involve the hydrogen atoms are neglected. The other parameter of the SPC/E model represented in Table 1 [55].

As mentioned before, the water/Fe_3O_4 nanofluid was simulated in our MD study. The atomic structure of water/Fe_3O_4 nanofluid with various numbers of Fe_3O_4 nanoparticles is depicted in Fig. 2. For MD simulation of Fe_3O_4 nanoparticles, there are several interatomic potentials such as Deriding, Universal Force Field (UFF), and Tersoff. Among these force fields, Tersoff is the best choice. The most common expression of the Tersoff potential is [58],

$$U = \frac{1}{2}\sum_i\sum_{i\neq j} V_{ij} \tag{12}$$

$$V_{ij} = f_C(r_{ij})[f_R(r_{ij}) + b_{ij}f_A(r_{ij})] \tag{13}$$

In Eq. (13), f_R is a two-body term, and f_A includes three-body interactions. The summations in the formula are over all neighbor's j, and k of atom i within a distance $r_c = R + D$. r_c is a cut off distance which determines the effect range of the atomic interaction. Finally, other atomic interactions between atoms in our MD simulations were defined by Dreiding potential [59]. After atomic modeling and interatomic potentials defining, to investigate the water/Fe_3O_4 nanofluid atomic manner in Cu microchannel, the density, velocity and temperature profiles are reported. The schematic of our MD simulation with various numbers of Fe_3O_4 nanoparticles and various radius of this nanoparticle depicted in Figs. 2 and 3, respectively. In our simulated atomic structures, the number of atoms in the simulation box and the accuracy of atomic interaction are the main limitations in which, by these parameters increasing, the simulation time increases, too.

3. Results and discussion

3.1. Total energy of simulated atomic structures

In the first step of our MD simulation, the total energy of the simulated structures is investigated. Fig. 4 shows this parameter variation for 1,000,000 time steps. From this figure, we can see the stability of our MD simulations. Physically, stability in atomic structures arises from the appropriate choice of atomic structure and interatomic force-fields. We can say that, by adding nanoparticle to water molecules, the total energy and atomic stability of simulated structures increases. Base on the fact that the total energy is equal to the sum of the potential and kinetic energy of the atomic structures, it can be concluded that the potential energy (negative quantity) is larger than the kinetic energy (positive quantity) in our simulated systems, which indicates the thermodynamic equilibrium of these structures. Furthermore, the maximum rate of the atomic system energy reported in Table 2 as a function of the Fe_3O_4 nanoparticles number. By increasing the number and radius of Fe_3O_4 nanoparticle, the total energy of atomic structure increases, and the maximum rate of this parameter reaches −753,366 eV from −681,027 eV (Table 3). This manner shows that, by adding nanoparticles to base fluid, the attraction force in fluid atomic structure rises, and so the stability of these structures improves. In the next steps of our theoretical study, we report the density, velocity, and temperature profiles of water/ Fe_3O_4 nanofluid.

3.2. Density profile of simulated atomic structures

The density profile of nanofluid particles shows the atomic manner of these structures in an ideal microchannel. So this physical parameter has high importance for atomic analysis of these structures. In order to compute the density profile of water/ Fe_3O_4 nanofluid in Cu microchannel, the microchannel divided into 1888 identical bins. Geometrically, in our simulated structures, each bin has $L_x \times L_z \times \Delta y$ volume, where L_x and L_z are the microchannel lengths in x and z directions, and Δy is equal to L_y/N_{bin}, which N_{bin} is the number of bins. Fig. 5 shows the distribution of water/ Fe_3O_4 nanofluid atoms in the microchannel as a function of nanoparticle's number in the base fluid

Table 1
The ε and σ parameters for LJ interaction for SPC/E model of water molecules [55].

Element	σ(Å)	ε (kcal/mol)
O	3.166	0.1553
H	0.0	0.0

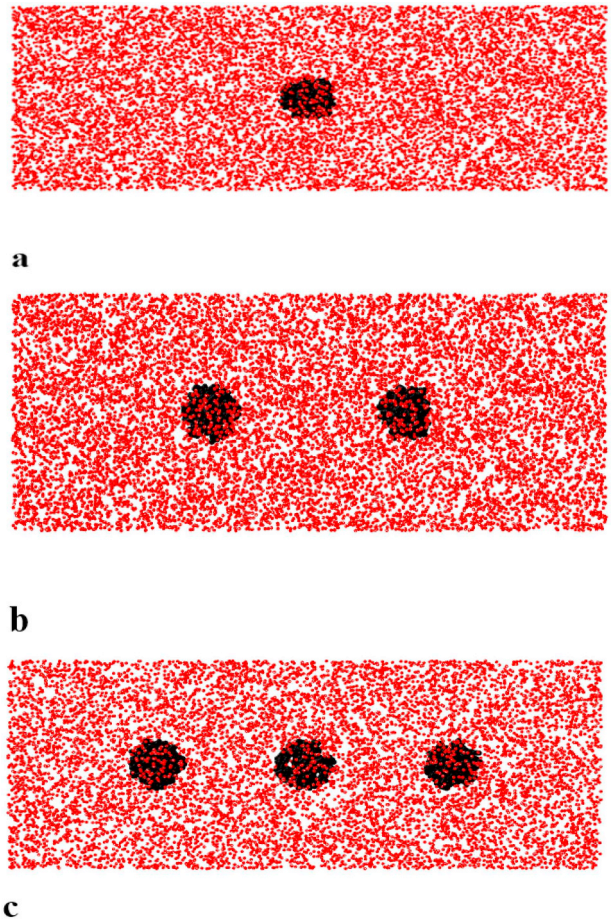

Fig. 2. Schematic of water/Fe_3O_4 nanofluid with various number of Fe_3O_4 nanoparticles, a) 1, b) 2, and c) 3 nanoparticles.

(water). From this figure, it can be seen that the fluid atoms absorbed by microchannel walls and so the atomic density rate of nanofluid has a maximum rate in these areas. Furthermore, the atomic density rate of water/ Fe_3O_4 nanofluid decreases in the middle bins of Cu microchannel. By increasing the Fe_3O_4 nanoparticles, which added to water fluid, the density profile of simulated structures rises. Numerically, by increasing nanoparticles number from 1 to 3, the maximum rate of nanofluid density changes from 1.396 g/cm^3 to 1.675 g/cm^3 (Table 4). Furthermore, base on Fig. 6 and Table 5, by increasing the radius of Fe_3O_4 nanoparticle from 25 nm to 75 nm, the maximum rate of density reached to 1.396 g/cm^3 and 1.508 g/cm^3, respectively. Physically, by adding nanoparticle to base fluid, the interatomic potentials go to a negative rate and so attraction force between microchannel and nanofluid increases. So, we can conclude that, by increasing Fe and O atoms in simulated nanofluid, density of this atomic structure in Cu microchannel increased, and it should be considered in practical applications.

3.3. Velocity profile of simulated atomic structures

The velocity of water/ Fe_3O_4 nanofluids atoms shows the dynamical manner of these atoms as a function of MD simulation time. To report the velocity distribution of water/ Fe_3O_4 nanofluid atoms in ideal Cu microchannel, the velocity of each particle calculated, and the time averaging of these calculations, are reported in Fig. 7. This figure shows the velocity distribution of nanofluid with various numbers of nanoparticles in a microchannel. From this figure, we can say that the velocity rate is maximum in the middle bins of the microchannel. In these bins, the interaction between Cu atoms and nanofluid particles has the minimum rate, and so the water/ Fe_3O_4 nanofluid is moving arbitrarily.

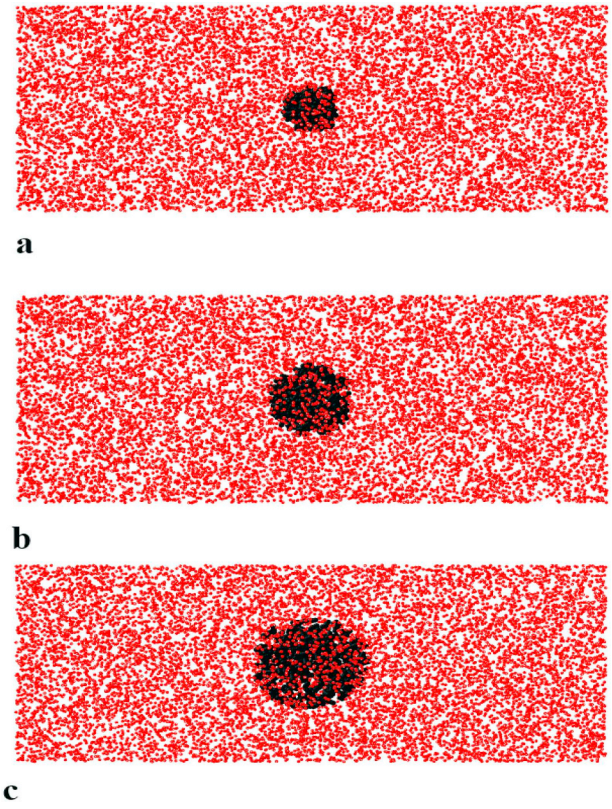

Fig. 3. Schematic of water/Fe_3O_4 nanofluid with various nanoparticle radius, a) 25 nm, b) 50 nm, and c) 75 nm.

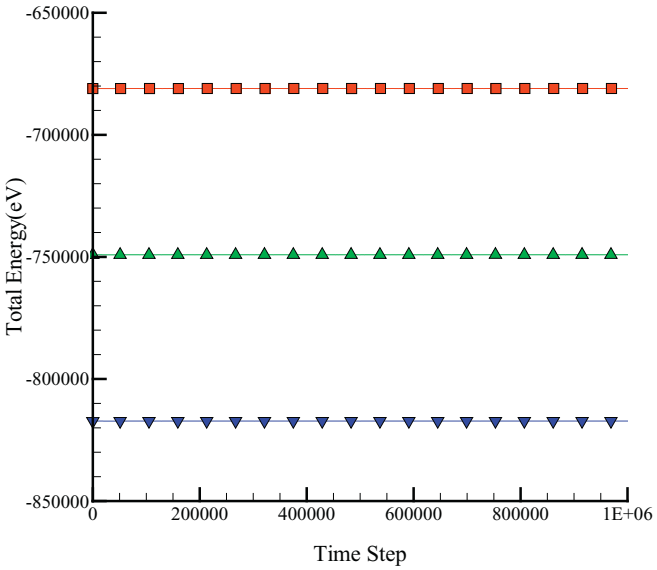

Fig. 4. Total energy of water/Fe_3O_4 nanofluid with various number of Fe_3O_4 nanoparticles as a function of simulation time step.

Table 2
The total energy rate of water/Fe_3O_4 nanofluid as a function of Fe_3O_4 nanoparticle number in 1,000,000 time step.

Number of nanoparticles	Energy(eV)
1 NP	−681,027
2 NP	−749,130
3 NP	−817,232

Table 3
The total energy rate of water/Fe_3O_4 nanofluid as a function of Fe_3O_4 nanoparticle radius in 1,000,000 time step.

Radius of nanoparticles(nm)	Energy(eV)
25	−681,027
50	−712,369
75	−753,366

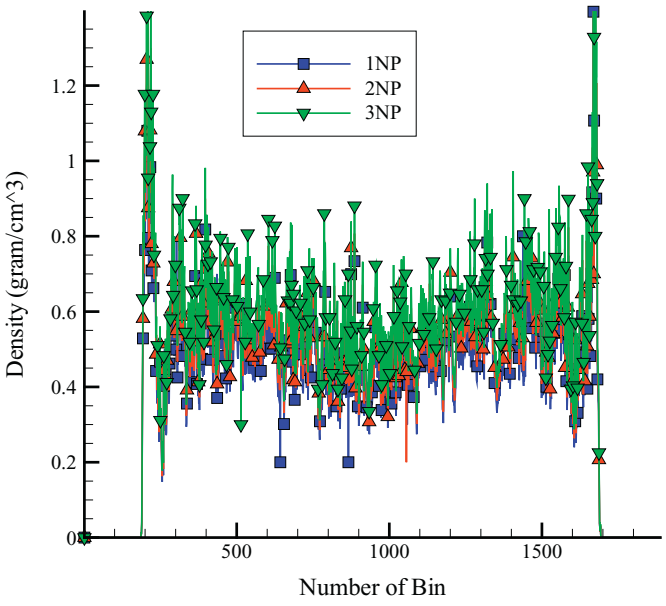

Fig. 5. Density profile of water/ Fe_3O_4 nanofluid as a function of Fe_3O_4 nanoparticle's number.

Table 4
Maximum rate of density in water/ Fe_3O_4 nanofluid by various number of Fe_3O_4 nanoparticles.

Number of nanoparticles	Density(gram/cm^3)
1 NP	1.396
2 NP	1.536
3 NP	1.675

Furthermore, this dynamical parameter is minimized in the first and final bins of a microchannel. This manner shows the Poiseuille flow manner of water/ Fe_3O_4 nanofluid atoms in ideal Cu microchannel. By adding Fe_3O_4 nanoparticles to base fluid, the velocity of water/ Fe_3O_4 nanofluid increases. From Table 6, the maximum velocity rate of water/ Fe_3O_4 nanofluid with one nanoparticle is 0.0068 *Å*/ps, by adding two more Fe_3O_4 nanoparticles to initial nanofluid, the velocity rises to 0.0117 *Å*/ps. Fe_3O_4 nanoparticle radius increasing has a similar effect on the velocity profile of water/ Fe_3O_4 nanofluid. By nanoparticle radius increasing from 25 nm to 75 nm, the mobility of the atomic structure increases. From Fig. 8 and Table 7, the maximum rate of atomic velocity increases from 0.0068 *Å*/ps to 0.0089 *Å*/ps by increasing Fe_3O_4 nanoparticle's radius. Physically, according to these results, we can say that, by increasing the Fe_3O_4 atom numbers in water/ Fe_3O_4 nanofluid, the effective force which is implemented to nanofluid atoms from microchannel walls decreases and so the atomic velocity of water/ Fe_3O_4 nanofluids increases. In other words, by adding nanoparticles to base fluid, the attraction between microchannel atoms and their adjacent nanofluid atoms increases. By this attraction force increasing, the mobility of middle nanofluid atoms increases, and these particles can freely move.

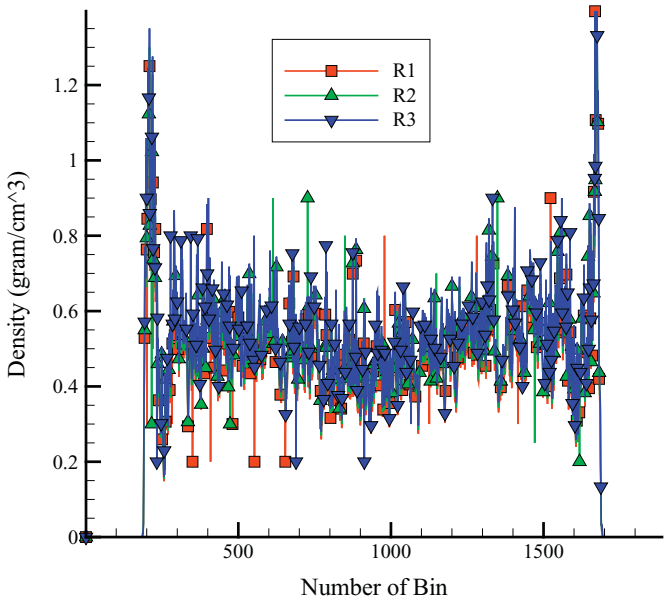

Fig. 6. Density profile of water/Fe3O4 nanofluid as a function of Fe_3O_4 nanoparticle's radius.

Table 5
Maximum rate of density in water/ Fe_3O_4 nanofluid by various radiuses of Fe_3O_4 nanoparticles.

Radius of nanoparticles(nm)	Density(gram/cm^3)
25	1.396
50	1.452
75	1.508

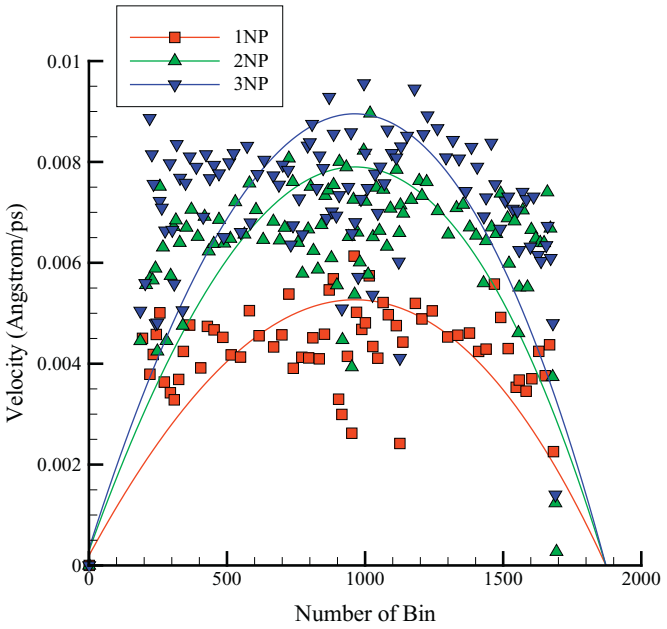

Fig. 7. Velocity profile of water/ Fe_3O_4 nanofluid as a function of Fe_3O_4 nanoparticle's number.

3.4. Temperature profile of simulated atomic structures

The thermodynamic properties of nanofluid structures have important effects on their function in industrial applications. In the final section of our research, we report that how the temperature of water/

Table 6
Maximum rate of velocity in water/ Fe_3O_4 nanofluid by various number of Fe_3O_4 nanoparticle.

Number of nanoparticles	Velocity(A/ps)
1 NP	0.0068
2 NP	0.0102
3 NP	0.0116

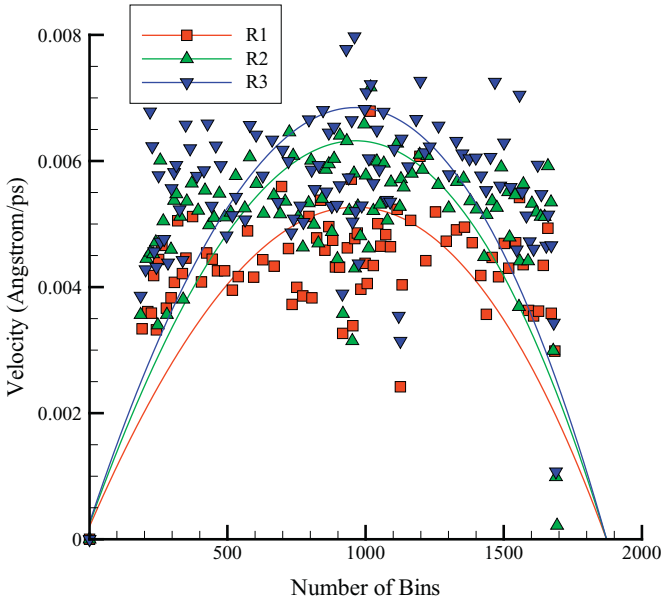

Fig. 8. Velocity profile of water/ Fe_3O_4 nanofluid as a function of Fe_3O_4 nanoparticle's radius.

Table 7
Maximum rate of velocity in water/ Fe_3O_4 nanofluid by various radius of Fe_3O_4 nanoparticle.

Radius of nanoparticles(nm)	Velocity(A/ps)
25	0.0068
50	0.0082
75	0.0089

Fe_3O_4 nanofluid atoms is distributed in an ideal microchannel. To obtain the temperature profile, similar to velocity section, the average temperature of water/ Fe_3O_4 nanofluid atoms is calculated in every 1888 bins and in every 1000 time steps. Fig. 9 shows the number of Fe_3O_4 nanoparticle effects on the water/ Fe_3O_4 nanofluid temperature profile. As depicted in this figure, the Poiseuille flow has a quadratic temperature profile, and the maximum rate of temperature occurs in the middle bins of an ideal microchannel. From Fig. 10, we can say that the atomic temperature of water/ Fe_3O_4 nanofluid atoms increases by Fe_3O_4 adding nanoparticle to fluid atoms. Numerically, the maximum rate of temperature varies from 593 K to 712 K by increasing the number of nanoparticles from 1 to 3 as reported in Table 8. These phenomena occur because the nanoparticles have high temperatures rather than base fluid atoms. The radius of Fe_3O_4 nanoparticles has an identical effect on water/ Fe_3O_4 nanofluid temperature as depicted in Fig. 10. By increasing the radius of Fe_3O_4 nanoparticles from 25 nm to 75 nm, the maximum rate of water/ Fe_3O_4 nanofluid maximum temperature increases from 593 K to 641 K (Table 9). The maximum temperature increasing of water/ Fe_3O_4 nanofluid from 593 K to 712 K physically arises from inserting force to atoms. This external parameter causes more movements of nanofluid atoms, and from $\frac{1}{2}\ mv^2 = 3/2\ k_BT$, the temperature of nanofluid increases. Physically, by adding

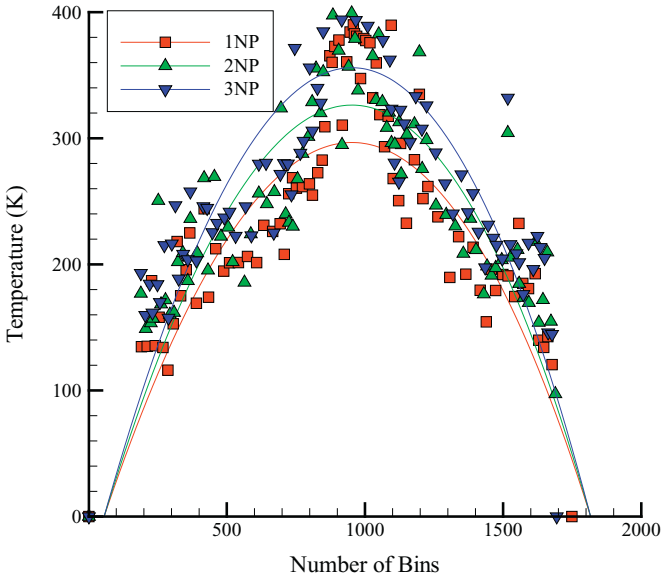

Fig. 9. Temperature profile of water/ Fe_3O_4 nanofluid as a function of Fe_3O_4 nanoparticle's number.

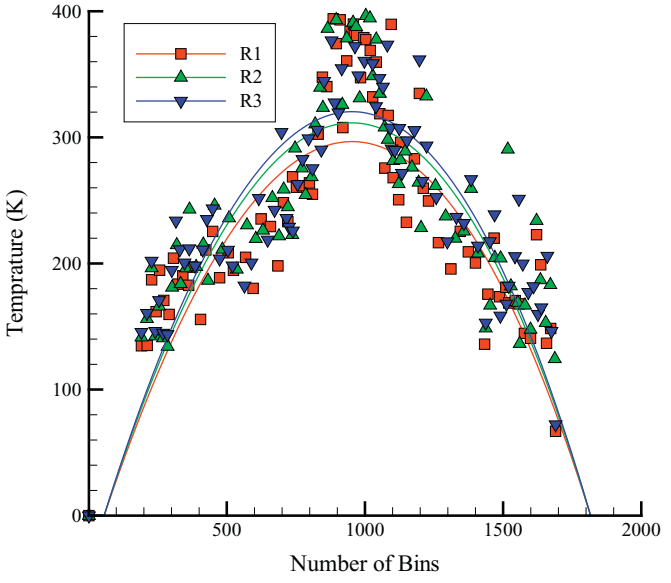

Fig. 10. Temperature profile of water/ Fe_3O_4 nanofluid as a function of Fe_3O_4 nanoparticle's radius.

Table 8
Maximum rate of temperature in water/ Fe_3O_4 nanofluid by various number of Fe_3O_4 nanoparticle.

Number of nanoparticles	Temperature(K)
1 NP	593
2 NP	653
3 NP	712

nanoparticles to base fluid, the mobility and so temperature of middle nanofluid atoms increases. In this section, we note that maximum temperature of the particles is 712 K, and many of the nanofluid atoms have lesser temperature according to Figs. 9 and 10.

Table 9
Maximum rate of temperature in water/ Fe_3O_4 nanofluid by various radius of Fe_3O_4 nanoparticle.

Radius of nanoparticles (nm)	Temperature (K)
25	593
50	623
75	641

4. Conclusion

In the actual electronic apparatus, the electric field presence in structure and so this parameter affects different parts of the apparatus. One of the most important parts of an electronic apparatus is its cooling system, which today, nanofluids implemented for these parts. In this computational study, we use a molecular dynamics approach to calculate the atomic manner of water/Fe3O4 nanofluid in ideal Cu microchannel at 300 K in the presence of an external electric field. In our simulations, the number of Fe_3O_4 nanoparticles varies from 1 to 3 nanoparticles. Furthermore, Fe_3O_4 nanoparticle radius increasing has identical effects. Finally, our conclusions from our computational study are as following:

A. Number of Fe_3O_4 nanoparticles within the water fluid is an important factor in water/ Fe_3O_4 nanofluid density. In our molecular dynamics simulations, the maximum rate of density was calculated for nanofluid by 3 nanoparticles with 1.675 g/cm^3 rate.
B. Molecular dynamics results showed that the Fe_3O_4 nanoparticle size increasing, affected on the total density of water/ Fe_3O_4 nanofluid.
C. In simulated structures, atomic velocity of water/ Fe_3O_4 nanofluid has a direct relation with Fe_3O_4 nanoparticle number. Maximum rate of velocity in water/ Fe_3O_4 nanofluid rises to 0.0116 Å/ps by adding three nanoparticles to base fluid.
D. Maximum velocity rate of water/ Fe_3O_4 nanofluid increases from 0.0068 Å /ps to 0.0089 Å/ps by radius of nanoparticle increasing from 25 nm to 75 nm.
E. By adding Fe_3O_4 nanoparticle to water fluid, the atomic temperature of nanofluid increases. Numerically, maximum temperature of nanofluid is calculated for atomic structure by 3 nanoparicle with 712 K rate.
F. Increasing Fe_3O_4 nanoparticle radius changes the temperature of water/ Fe_3O_4 nanofluid from 593 K to 641 K.

Author statement

- The corresponding author is responsible for ensuring that the descriptions are accurate and agreed by all authors.
- The role(s) of all authors are listed.
- Authors have contributed in multiple roles.

Declaration of Competing Interest

The authors declare that they have no known competing financial interests or personal relationships that could have appeared to influence the work reported in this paper.

References

[1] Y. Orooji, M. Ghanbari, O. Amiri, M. Salavati-Niasari, Facile fabrication of silver iodide/graphitic carbon nitride nanocomposites by notable photo-catalytic performance through sunlight and antimicrobial activity, Journal of Hazardous Materials 389 (2020) 122079, , https://doi.org/10.1016/j.jhazmat.2020.122079.
[2] Y. Orooji, R. Mohassel, O. Amiri, A. Sobhani, M. Salavati-Niasari, Gd2ZnMnO6/ZnO nanocomposites: Green sol-gel auto-combustion synthesis, characterization and photocatalytic degradation of different dye pollutants in water, Journal of Alloys and Compounds (2020) 155240, , https://doi.org/10.1016/j.jallcom.2020.155240.
[3] Y. Orooji, M.H. Irani-nezhad, R. Hassandoost, A. Khataee, S.R. Pouran, S.W. Joo, Cerium doped magnetite nanoparticles for highly sensitive detection of metronidazole via chemiluminescence assay, Spectrochimica Acta Part A: Molecular and Biomolecular Spectroscopy (2020) 118272, , https://doi.org/10.1016/j.saa.2020.118272.
[4] P. Mehdizadeh, Y. Orooji, O. Amiri, M. Salavati-Niasari, H. Moayedi, Green synthesis using cherry and orange juice and characterization of TbFeO3 ceramic nanostructures and their application as photocatalysts under UV light for removal of organic dyes in water, Journal of Cleaner Production 252 (2020) 119765, , https://doi.org/10.1016/j.jclepro.2019.119765.
[5] S.U.S. Choi, Jeffrey Eastman, Enhancing thermal conductivity of fluids with nanoparticles, Proceedings of the ASME International Mechanical Engineering Congress and Exposition, 66 1995.
[6] M. Hashemian, S. Jafarmadar, J. Nasiri, H. Sadighi Dizaji, Enhancement of heat transfer rate with structural modification of double pipe heat exchanger by changing cylindrical form of tubes into conical form, Appl. Therm. Eng. 118 (2017) 408–417, https://doi.org/10.1016/j.applthermaleng.2017.02.095.
[7] J.C. Maxwell, A Treatise on Electricity and Magnetism, Clarendon Press, Oxford, UK, 1891.
[8] S.U.S. Choi, Y.I. Cho, K.E. Kasza, Degradation effects of dilute polymer solutions on turbulent friction and heat transfer behavior, J. Non-Newtonian Fluid Mech. 41 (3) (1992) 289–307, https://doi.org/10.1016/0377-0257(92)87003-t.
[9] U. Choi, D.M. France, B.D. Knodel, Impact of Advanced Fluids on Costs of District Cooling Systems, Argonne National Lab, 1992.
[10] U. Choi, T. Tran, Experimental studies of the effects of non-Newtonian surfactant solutions on the performance of a shell-and-tube heat exchanger, Recent Developments in Non-Newtonian Flows and Industrial Applications, The American Society of Mechanical Engineers, New York, NY, USA, 1991.
[11] K. Liu, U. Choi, K.E. Kasza, Measurements of Pressure Drop and Heat Transfer in Turbulent Pipe Flows of Particulate Slurries, Argonne National Lab, 1988.
[12] Y. Xuan, Q. Li, Heat transfer enhancement of nanofluids, Int. J. Heat Fluid Flow 21 (1) (2000) 58–64, https://doi.org/10.1016/s0142-727x(99)00067-3.
[13] N. Ali, J.A. Teixeira, A. Addali, A review on nanofluids: fabrication, stability, and thermophysical properties, J. Nanomater. 2018 (2018) 1–33, https://doi.org/10.1155/2018/6978130.
[14] M. Ghasemi, A. Khataee, P. Gholami, R.D.C. Soltani, A. Hassani, Y. Orooji, In-situ electro-generation and activation of hydrogen peroxide using a CuFeNLDH-CNTs modified graphite cathode for degradation of cefazolin, Journal of Environmental Management 267 (2020) 110629, , https://doi.org/10.1016/j.jenvman.2020.110629.
[15] T.D. Wheeler, A.D. Stroock, The transpiration of water at negative pressures in a synthetic tree, Nature 455 (7210) (2008) 208–212, https://doi.org/10.1038/nature07226.
[16] M. Whitby, N. Quirke, Fluid flow in carbon nanotubes and nanopipes, Nat. Nanotechnol. 2 (2) (2007) 87–94, https://doi.org/10.1038/nnano.2006.175.
[17] G.M. Whitesides, The origins and the future of microfluidics, Nature 442 (7101) (2006) 368–373, https://doi.org/10.1038/nature05058.
[18] Y. Xu, N.R. Aluru, Carbon nanotube screening effects on the water-ion channels, Appl. Phys. Lett. 93 (4) (2008) 043122, , https://doi.org/10.1063/1.2963975.
[19] S.C. Yang, Effects of surface roughness and interface wettability on nanoscale flow in a nanochannel, Microfluid. Nanofluid. 2 (6) (2006) 501–511, https://doi.org/10.1007/s10404-006-0096-5.
[20] L. Yang, S. Garde, Modeling the selective partitioning of cations into negatively charged nanopores in water, J. Chem. Phys. 126 (8) (2007) 084706, , https://doi.org/10.1063/1.2464083.
[21] Z. Yao, J.-S. Wang, G.-R. Liu, M. Cheng, Improved neighbor list algorithm in molecular simulations using cell decomposition and data sorting method, Comput. Phys. Commun. 161 (1–2) (2004) 27–35, https://doi.org/10.1016/j.cpc.2004.04.004.
[22] H. Zhang, J.F. Ely, AUA model NEMD and EMD simulations of the shear viscosity of alkane and alcohol systems, Fluid Phase Equilib. 217 (1) (2004) 111–118, https://doi.org/10.1016/j.fluid.2003.11.002.
[23] G.P. Berman, F.M. Izrailev, The Fermi–Pasta–Ulam problem: fifty years of progress, Chaos 15 (1) (2005) 015104, , https://doi.org/10.1063/1.1855036.
[24] B.J. Alder, T.E. Wainwright, Studies in molecular dynamics. I. General method, J. Chem. Phys. 31 (2) (1959) 459, https://doi.org/10.1063/1.1730376.
[25] A. Rahman, Correlations in the motion of atoms in liquid argon, Phys. Rev. 136 (2A) (19 October 1964) A405–A411 Bibcode:1964PhRv..136..405R https://doi.org/10.1103/PhysRev.136.A405.
[26] B.J. Alder, T.E. Wainwright, Studies in molecular dynamics. I. General method, J. Chem. Phys. 31 (2) (1959) 459 Bibcode:1959JChPh..31..459A https://doi.org/10.1063/1.1730376.
[27] N.A. Jolfaei, N.A. Jolfaei, M. Hekmatifar, A. Piranfar, D. Toghraie, R. Sabetvand, S. Rostami, Investigation of thermal properties of DNA structure with precise atomic arrangement via equilibrium and non-equilibrium molecular dynamics approaches, Comput. Methods Prog. Biomed. 105169 (2019), https://doi.org/10.1016/j.cmpb.2019.105169.
[28] R. Sabetvand, M.E. Ghazi, M. Izadifard, Studying temperature effects on electronic and optical properties of cubic CH3NH3SnI3 perovskite, J. Comput. Electron. (2020), https://doi.org/10.1007/s10825-020-01443-3.
[29] N.A. Jolfaei, N.A. Jolfaei, M. Hekmatifar, A. Piranfar, D. Toghraie, R. Sabetvand, S. Rostami, Investigation of thermal properties of DNA structure with precise atomic arrangement via equilibrium and non-equilibrium molecular dynamics approaches, Comput. Methods Prog. Biomed. 105169 (2019), https://doi.org/10.1016/j.cmpb.2019.105169.
[30] M. Goel, S.P. Harsha, S. Singh, A.K. Sahani, Analysis of temperature, helicity and size effect on the mechanical properties of carbon nanotubes using molecular

dynamics simulation, Mater. Today (2020), https://doi.org/10.1016/j.matpr.2020.01.130.
[31] D. Toghraie, M. Hekmatifar, Y. Salehipour, M. Afrand, Molecular dynamics simulation of Couette and Poiseuille water-copper nanofluid flows in rough and smooth nanochannels with different roughness configurations, Chem. Phys. 527 (2019) 110505, https://doi.org/10.1016/j.chemphys.2019.110505.
[32] A.R. Albooyeh, A. Dadrasi, A.H. Mashhadzadeh, Effect of point defects and low-density carbon-doped on mechanical properties of BNNTs: a molecular dynamics study, Mater. Chem. Phys. 239 (2020) 122107, https://doi.org/10.1016/j.matchemphys.2019.122107.
[33] Y. Peng, M. Zarringhalam, M. Hajian, D. Toghraie, S.J. Tadi, M. Afrand, Empowering the boiling condition of Argon flow inside a rectangular microchannel with suspending Silver nanoparticles by using of molecular dynamics simulation, J. Mol. Liq. 111721 (2019), https://doi.org/10.1016/j.molliq.2019.111721.
[34] Y. Peng, M. Zarringhalam, A.A. Barzinjy, D. Toghraie, M. Afrand, Effects of surface roughness with the spherical shape on the fluid flow of Argon atoms flowing into the microchannel, under boiling condition using molecular dynamic simulation, J. Mol. Liq. 111650 (2019), https://doi.org/10.1016/j.molliq.2019.111650.
[35] M. Zarringhalam, H. Ahmadi-Danesh-Ashtiani, D. Toghraie, R. Fazaeli, A statistical method for simulation of boiling flow inside a Platinum microchannel, Physica A (2019) 123879, https://doi.org/10.1016/j.physa.2019.123879.
[36] M. Hadipeykani, F. Aghadavoudi, D. Toghraie, A molecular dynamics simulation of the glass transition temperature and volumetric thermal expansion coefficient of thermoset polymer based epoxy nanocomposite reinforced by CNT: a statistical study, Physica A (2020) 123995, https://doi.org/10.1016/j.physa.2019.123995.
[37] S.-R. Yan, N. Shirani, M. Zarringhalam, D. Toghraie, Q. Nguyen, A. Karimipour, Prediction the boiling flow characteristics in rough and smooth microchannels using of molecular dynamics simulation: investigation the effects of boundary wall temperatures, J. Mol. Liq. 112937 (2020), https://doi.org/10.1016/j.molliq.2020.112937.
[38] M. Miansari, H. Aghajani, M. Zarringhalam, D. Toghraie, Numerical study on the effects of geometrical parameters and Reynolds number on the heat transfer behavior of carboxy-methyl cellulose/CuO non-Newtonian nanofluid inside a rectangular microchannel, J. Therm. Anal. Calorim. (2020), https://doi.org/10.1007/s10973-020-09447-8.
[39] S. Witharana, H. Chen, Y. Ding, Stability of nanofluids in quiescent and shear flow fields, Nanoscale Res. Lett. 6 (2011) 231 http://www.nanoscalereslett.com/content/6/1/231.
[40] H. Chen, S. Witharana, et al., Predicting thermal conductivity of liquid suspensions of nanoparticles (nanofluids) based on Rheology, Particuology 7 (2) (2009) 151–157, https://doi.org/10.1016/j.partic.2009.01.005.
[41] B. Karbasifar, M. Akbari, D. Toghraie, Mixed convection of Water-Aluminum oxide nanofluid in an inclined lid-driven cavity containing a hot elliptical centric cylinder, Int. J. Heat Mass Transf. 116 (2018) 1237–1249, https://doi.org/10.1016/j.ijheatmasstransfer.2017.09.110.
[42] M. Gholami, M.R. Nazari, M.H. Talebi, F. Pourfattah, O.A. Akbari, D. Toghraie, Natural convection heat transfer enhancement of different nanofluids by adding dimple fins on a vertical channel wall, Chin. J. Chem. Eng. (2019), https://doi.org/10.1016/j.cjche.2019.11.001.
[43] W. He, D. Toghraie, A. Lotfipour, F. Pourfattah, A. Karimipour, M. Afrand, Effect of twisted-tape inserts and nanofluid on flow field and heat transfer characteristics in a tube, Int. Commun. Heat Mass Transfer 110 (2020) 104440, https://doi.org/10.1016/j.icheatmasstransfer.2019.104440.
[44] F. Pourfattah, M. Sabzpooshani, Ö. Bayer, D. Toghraie, A. Asadi, On the optimization of a vertical twisted tape arrangement in a channel subjected to MWCNT–water nanofluid by coupling numerical simulation and genetic algorithm, J. Therm. Anal. Calorim. (2020), https://doi.org/10.1007/s10973-020-09490-5.
[45] E. Khodabandeh, R. Boushehri, O.A. Akbari, S. Akbari, D. Toghraie, Numerical investigation of heat and mass transfer of water—silver nanofluid in a spiral heat exchanger using a two-phase mixture method, J. Therm. Anal. Calorim. (2020), https://doi.org/10.1007/s10973-020-09533-x.
[46] W.H. Press, S.A. Teukolsky, W.T. Vetterling, B.P. Flannery, “Section 17.4. Second-order Conservative Equations”. Numerical Recipes: The Art of Scientific Computing, 3rd ed., Cambridge University Press, New York, 2007 (ISBN 978-0-521-88068-8).
[47] Ernst Hairer, Christian Lubich, Gerhard Wanner, Geometric numerical integration illustrated by the Störmer/Verlet method, Acta Numerica 12 (2003) 399–450 Bibcode:2003AcNum..12..399H. CiteSeerX 10.1.1.7.7106 https://doi.org/10.1017/S0962492902000144.
[48] S. Plimpton, Fast parallel algorithms for short-range molecular dynamics, J. Comput. Phys. 117 (1) (1995) 1–19, https://doi.org/10.1006/jcph.1995.1039.
[49] S.J. Plimpton, A.P. Thompson, Computational aspects of many-body potentials, MRS Bull. 37 (5) (2012) 513–521, https://doi.org/10.1557/mrs.2012.96.
[50] W.M. Brown, P. Wang, S.J. Plimpton, A.N. Tharrington, Implementing molecular dynamics on hybrid high performance computers – short range forces, Comput. Phys. Commun. 182 (4) (2011) 898–911, https://doi.org/10.1016/j.cpc.2010.12.021.
[51] A. Stukowski, Visualization and analysis of atomistic simulation data with OVITO–the Open Visualization Tool, Model. Simul. Mater. Sci. Eng. 18 (1) (2009) 015012, , https://doi.org/10.1088/0965-0393/18/1/015012.
[52] S. Nosé, A unified formulation of the constant temperature molecular-dynamics methods, J. Chem. Phys. 81 (1) (1984) 511–519 Bibcode:1984JChPh..81..511N https://doi.org/10.1063/1.447334.
[53] William G. Hoover, Canonical dynamics: equilibrium phase-space distributions, Phys. Rev. A 31 (3) (Mar 1985) 1695–1697 Bibcode:1985PhRvA..31.1695H https://doi.org/10.1103/PhysRevA.31.1695.
[54] William G. Hoover, Brad Lee Holian, Kinetic moments method for the canonical ensemble distribution, Phys. Lett. A 211 (5) (1996-02-26) 253–257 Bibcode:1996PhLA..211..253H. CiteSeerX 10.1.1.506.9576 https://doi.org/10.1016/0375-9601(95)00973-6.
[55] K. Toukan, A. Rahman, Molecular-dynamics study of atomic motions in water, Phys. Rev. B 31 (5) (1985) 2643–2648 Bibcode:1985PhRvB..31.2643T https://doi.org/10.1103/PhysRevB.31.2643. PMID 9936106.
[56] H.J.C. Berendsen, J.R. Grigera, T.P. Straatsma, The missing term in effective pair potentials, J. Phys. Chem. 91 (24) (1987) 6269–6271, https://doi.org/10.1021/j100308a038.
[57] J.E. Lennard-Jones, On the determination of molecular fields, Proc. R. Soc. Lond. A 106 (738) (1924) 463–477 Bibcode:1924RSPSA.106..463J https://doi.org/10.1098/rspa.1924.0082.
[58] J. Tersoff, New empirical approach for the structure and energy of covalent systems, Phys. Rev. B 37 (12) (1988) 6991–7000, https://doi.org/10.1103/physrevb.37.6991.
[59] S.L. Mayo, B.D. Olafson, W.A. Goddard, DREIDING: a generic force field for molecular simulations, J. Phys. Chem. 94 (26) (1990) 8897–8909, https://doi.org/10.1021/j100389a010.